

Derailment Assessment using FBG

Ajit Kumar

Department of Electronics and communication, Bit Mesra, Ranchi-835215

Email: ajitk9kumar@gmail.com

Abstract -This paper proposes the use of FBG sensor to measure the lateral and vertical forces at the flange contact point. The ratio of lateral and vertical force at the rail-wheel contact point is called Nadal limit for a certain critical value which decides the derailment. Simulation has been done for the measurement of lateral and vertical forces with the increasing velocity and taking the range of radius of curvature from 600m to 1000m.

Keywords- Fiber Bragg Grating, Nadal’s limit, flange climb derailment, curve negotiation

1. INTRODUCTION

Derailment is an accident in railways, where a carriage, or part or the entire train, leaves the tracks on which it is travelling. Every year this problem leads to loss of lives and property. Hence it has become important to propose a monitoring method for the derailment assessment. Many authors have reported the use of conventional sensors in this regard. Akira Matsumoto et al. has reported the use of magnetostrictive displacement sensors for the measurement of vertical contact forces [9]. Hiroaki Ishida et al. has reported the use of load cells and actuator for the measurement of lateral, vertical displacement and creep forces [7]. C. Hung has reported the use of MEMS acceleration sensor and MEMS angular velocity sensor for the detection of early sign of derailment [2]. But these conventional sensors can't be used in hazardous environment unlike FBG sensors. Although many fiber sensors are commercially available but they have certain disadvantages like low spatial resolution and complexity in interrogation of output signal. So in order to overcome these problems sensor based on Fiber Bragg gratin (FBGs) has been used in this paper. This paper proposes the use of FBG sensor to measure lateral and vertical forces. The ratio of lateral to vertical force (Derailment coefficient) for a certain critical at which derailment is likely to occur is called Nadal limit. Thus by finding the derailment coefficient a monitoring method for the derailment assessment has been introduced.

2. DERAILMENT ASSESSMENT USING FBG SENSOR

Derailment can be considered as a function of wheel load, lateral force, normal force and attack angle of the wheel contact with the rail [4]. Derailment can occur on curve track or straight track. To find the safety against flange climb derailment, Nadal proposed a theoretical estimation method based on the ratio of lateral to vertical force [4]. Railway derailment may occur due to Wheel flange climb, Gauge widening, Rail rollover, Track panel shift [10].

Derailment due to flange climb only has been discussed in this paper. Wheel flange climb derailment occurs when wheel Climb on the top of the railhead and then run over the rail.

Ajit kumar , ajitk9kumar@gmail.com

Wheel climb derailment generally occurs where the wheel experiences high lateral force in combination with circumstances where there is reduced vertical force on flanging wheel. The high lateral force is induced due to large angle of attack whereas vertical force is reduced when there is rough track or large track twist. So flange climb derailments mainly occur on curves. This lateral to vertical force ratio (Q/Y) depends on Curve radius, Wheel rail profiles, Bogie suspension characteristics, Train speed

The Fig.1 shows the lateral and vertical forces at the flange contact point.

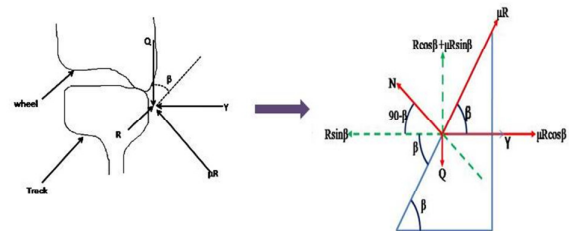


Figure1. Free body diagram for the estimation of Nadal ratio

In Fig.1 Y is lateral force, Q is vertical force and beta is flange angle at the contact point. The forces are resolved in X and Y axes giving the following equation

$$Y = R \sin \beta - \mu R \cos \beta \tag{1}$$

$$Q = R \cos \beta + \mu R \sin \beta . \tag{2}$$

Taking the ratio of both the equations and dividing the numerator and denominator of RHS part by Rcosbeta derailment coefficient is achieved

$$\frac{Y}{Q} = \frac{\tan \beta - \mu}{1 + \mu \tan \beta} \tag{3}$$

Where

mu =coefficient of friction between wheels and rail contact.

R= normal reaction force

μR = tangential friction force due to creep

Both R and μR varies as a function of Y. Climb does not occur with increasing Y till μR is saturated and flange contact slide down the rail. However for a certain critical value of Y/Q tangential friction is about to drop below its saturated value and flange climb occurs due to rolling instead of sliding.

Fig.2 shows the flow chart for derailment assessment. In this flow chart two cases one for straight track and another for curve track has been considered.

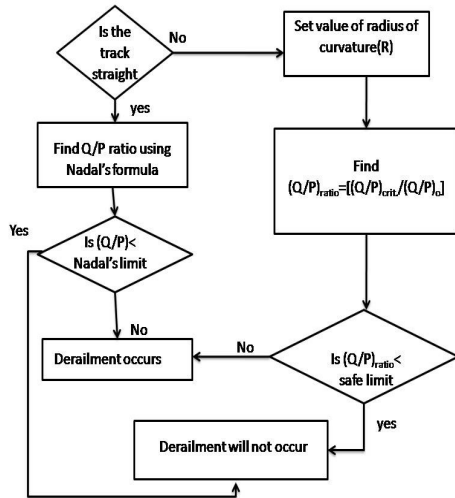


Figure2.Flow chart of Derailment assessment algorithm

For the straight track the radius of curve is infinite and so simply the vertical load and lateral forces have to be detected through shift in Bragg wavelength. For the curve track Wheel load varies due to Centrifugal force, Track twist, Torsion of secondary suspension spring whereas the Lateral force varies due to due to the reaction of inside friction force, centrifugal force and torsion of air suspension, track irregularities. So different analytical equation has been used for both the cases

But at last for both the cases the Q/P ratio has to be detected to get the safety against derailment ratio (Nadal ratio). The flow chart in Fig.3 shows the methodology to find vertical and lateral forces.

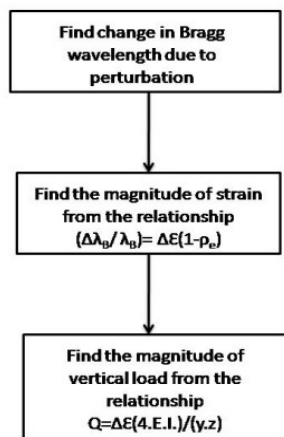


Figure3.Flow chart to detect vertical load of the wheel

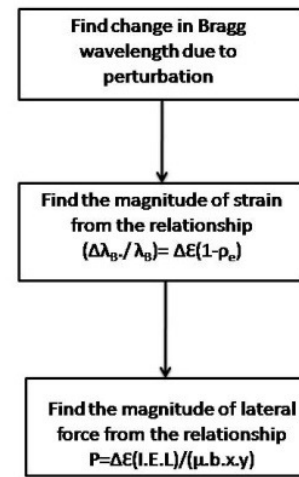


Figure4.Flow chart for the detection of lateral force

3. FBG SENSING PRINCIPLE

The working principle of FBG is based on the Fresnel's reflection of light centered at Bragg wavelength λ_B given by

$$\lambda_B = 2n\Lambda \tag{4}$$

Where n is the effective refractive index of the fiber core and Λ is the period of index modulation [3]. The wavelength shift $\Delta\lambda_B$ with respect to change in strain $\Delta\epsilon$ is given by the following relation

$$\frac{\Delta\lambda_B}{\lambda_B} = (1 - \rho)\Delta\epsilon \tag{5}$$

(5)

Where, ρ is the photo elastic coefficient of the fiber.

The reflected wavelength depends on the period of modulation as well as effective refractive index of the fiber. So when perturbation acts on fiber there is either compression or elongation of the FBG thereby changing the period of modulation and hence there is shift in Bragg wavelength. This shift in Bragg wavelength is used to find the magnitude of strain applied on FBG. The wavelength of the reflected light is detected and then transmitted to signal processing unit.

4. SET UP FOR THE MEASUREMENT OF VERTICAL AND LATERAL FORCES

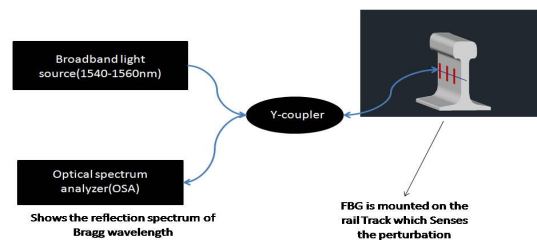


Figure5.Proposed setup

The proposed setup for the measurement of vertical and lateral forces as shown in Fig.5 consists of a Broadband

source which launches light into an array of FBGs, via a Y-coupler. The returned signal in the form of shift in Bragg wavelength from the FBGs is recorded on O.S.A

5. RESULTS AND DISCUSSION

Fig (6) shows the spectrum without load (red) and with load (black). The shift in Bragg wavelength is used to estimate the magnitude of applied lateral force. In the same manner when, the vertical load is applied, then there is a shift in the Bragg wavelength (Fig.8) thereby giving an estimate of the magnitude of vertical load.

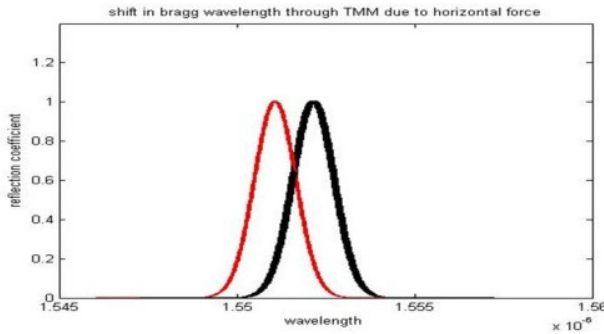


Figure6. Bragg Wavelength shift due to Lateral force

The Fig.7 shows the linear relationship between strain and the load.

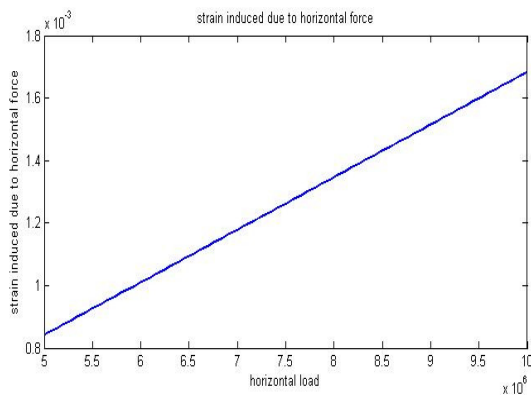


Figure7. Vertical strain due to horizontal load

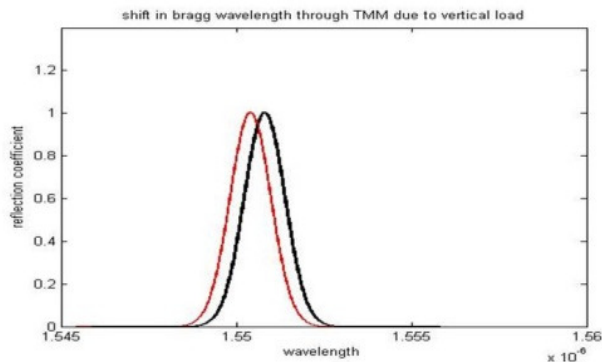


Figure8. Bragg wavelength shift due to vertical load

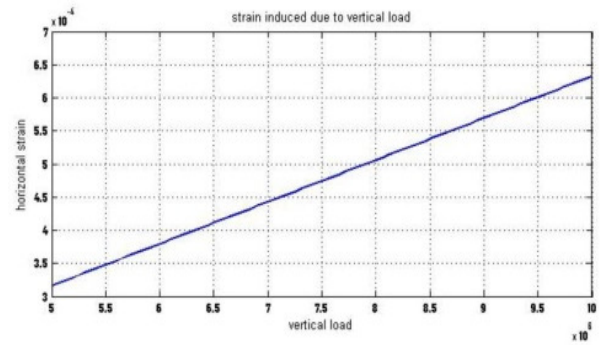


Figure9. Horizontal strain due to vertical load

The Fig 9 shows the horizontal strain induced due to vertical load. Similarly vertical strain induced due to horizontal strain is shown in Fig 7.

Once the magnitude of lateral force and vertical load has been extracted, the Nadal ratio can be calculated by finding their ratio

Simulation result has been derived for the assessment of derailment against curve radius and velocity of the train. This will help in track assessment when train passes through curve track.

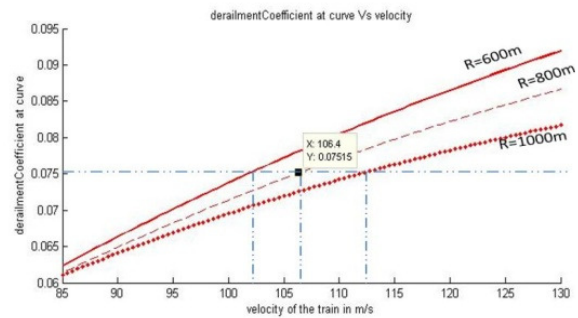


Figure10. Derailment coefficient for three radii at varying speeds

The Fig 10 shows derailment coefficient for three radius of curve (600m, 800,1000m) against velocity of the train. This Fig shows that derailment coefficient decreases as the radius increases making our assumption stronger that the probability of derailment is low on straight track (infinite radius). This Fig also shows that as the velocity (for a particular radius) is increasing, the derailment coefficient is increasing which proves that at higher velocity the probability of derailment is higher.

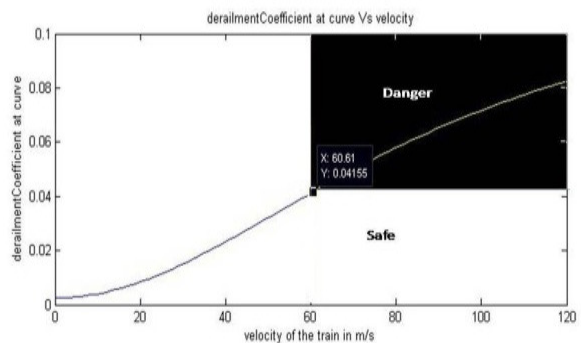


Figure11. Danger and Safe zones based on Nadal Limit taking 700m as radius of curve

Fig 11 results show the danger and safe zone for a particular radius (700m) of curve and velocity of the train. This Fig shows that the derailment coefficient is 0.04155 at velocity of 60.61m/s. It means that if train's speed exceed this speed for a 700m curve track then derailment is likely to occur.

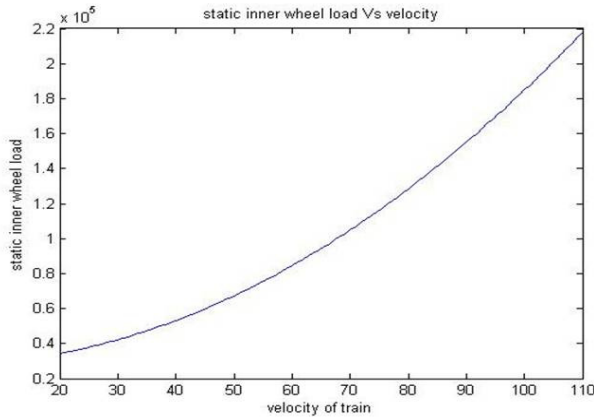


Figure12. Static inner wheel load of the leading axle

The Fig 12 shows how static inner wheel load of leading axle increases as the train passes through the curve.

Large angle of attack increases the probability of derailment as this increases the lateral force and reduces the vertical force.

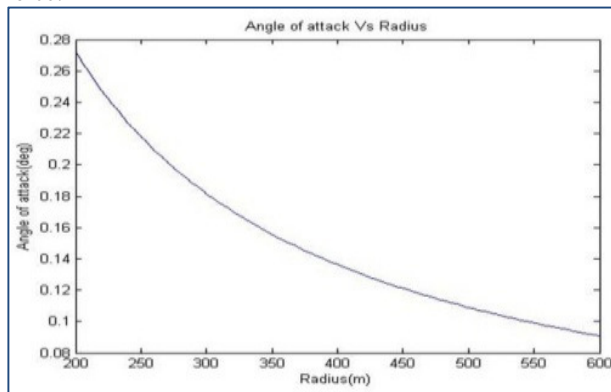


Figure13. Variation of Attack angle against Radius of curve

The Fig 13 shows that as the radius increases the angle of attack decreases so probability of derailment also decreases

6. EXPERIMENTAL RESULT

- Readings of performed experimental result
- Specification of rail model train
- Wheel separation= 7.5cm
- Radius at the curve= 27.1cm
- Total length of the track= 281.4cm

TABLE.1 Reading without load on the Train

Sr. No	Track	Velocity(c m/s)	λ_B (nm)-outer wheel/ λ_B (nm)-inner wheel	λ_r (nm)-outer wheel/ λ_r (nm)-inner wheel	$\Delta\lambda$ (nm)-outer wheel/ $\Delta\lambda$ (nm)-inner wheel
1.	Straight track down	26.04	1544.893	1544.869	0.025
2.	Straight track up	19.3	1544.880	1544.860	0.02
3.	Semicircular down	4.73	1544.844/1536.896	1544.824/1536.475	0.29/0.03
4.	Semicircular up	3.52	1544.882/1536.548	1544.840/1536.44	0.043/0.026

TABLE.2 Reading with load on the Train

Sr.No	Track	Velocity (cm/s)	λ_B (nm)-outer wheel/ λ_B (nm)-inner wheel	λ_r (nm)-outer wheel/ λ_r (nm)-inner wheel	$\Delta\lambda$ (nm)-outer wheel/ $\Delta\lambda$ (nm)-inner wheel
1.	Straight track down	27.65	1544.890	1544.842	0.048
2.	Straight track up	18.36	1544.890	1544.836	0.054
3.	Semicircular down	20.88	1544.896/1536.536	1544.85/1536.508	0.811/0.28
4.	Semicircular up	13.92	1544.896/1536.548	1544.854/1536.518	0.42/0.30

7. CONCLUSION

The application of forces were detected through FBG sensor and hence derailment coefficient ratio was estimated which gives the safety against wheel flange climb derailment.

REFERENCE

- [1] K. Y. Lee, K. K. Lee, S. L. Ho, "Exploration of Using FBG Sensor for Derailment Detector,". WSEAS Issue 6, Vol. 3, pp 2433-2447, 2004
- [2] C. Hung, Y. Shuda, M. Aki, T. Tsuji, M. Morikawa, T. Yamashita, T. Kawanabe, T. Kuimi, "Study on early signs of derailment for railway vehicles", vol.48, supplement, pp.451-466, 2010
- [3] Takai, H.; Uchida, M.; Muramatsu, H.; Ishida, H. "Derailment safety evaluation by analytical equations." Quarterly Report of RTRI . v. 43 no. 3 p. 119-124.
- [4] Marquis, B., and Grief, R., 2011, "Application of Nadal Limit in the Prediction of Wheel Climb Derailment," "Proceedings of the ASME/ASCE/IEEE 2011 Joint Rail Conference", Pueblo, CO, March 16-18, 2011, Paper No. JRC2011-56064.
- [5] Hiroaki Ishida, Takefumi Miyamoto, Eiichi Maebashi, Hisayo Doi, Kouhei Iida, Atsushi Furukawa, "Safety Assessment for Flange Climb Derailment of Trains Running at Low Speeds on Sharp Curves" QR of RTRI, Vol.47, No.2, May 2006
- [6] Chu-Liang Wei et.al, "A Fiber Bragg Grating Sensor System for Train Axle Counting", IEEE Sensors J. vol.10, No.12, pp.1905-1911, 2010
- [7] Hiroaki Ishida et.al, "Safety Assessment for Flange Climb Derailment of Trains Running at Low Speeds on Sharp Curves," QR of RTRI, vol.47, No.2, May 2006, pp.65-70.

- [9] Akira Matsumoto et.al. ,”Continuous observation of wheel/rail contact forces in curved track and theoretical consideration”, vehicle system dynamics, vol.50, supplement, pp.349-364, 2012
- [10] Huimin Wu, Nicholas Wilson, “Railway Vehicle Derailment and Prevention”,taylor & Francis Group, pp.209- 233, 2002.
- [11] I.Raman Kashyap, “Fiber Bragg Gratings,” *Academic Press*, 1999.
- [12] Turan Erdogan,” Fiber Grating Spectra”, journal of lightwave technology, vol. 15, no. 8, august 1997